Chem. Ber. **115**, 2153–2174 (1982)

Phosphinomethyl Complexes of Zirconium: A Molecular Orbital Study of Structure, Bonding and Reactivity Problems

Peter Hofmann *[1a], *Peter Stauffert*[1a], and *Neil E. Schore*[1b]

Institut für Organische Chemie, Universität Erlangen-Nürnberg, Henkestr. 42, D-8520 Erlangen, and

Department of Chemistry, University of California, Davis, Davis, California 95616, USA

Received October 27, 1981

The electronic structure and geometry of bent sandwich phosphinomethyl complexes of Zr^{IV} and Zr^{III} have been investigated by means of molecular orbital calculations. A fragment MO approach and perturbation arguments are utilized to explain the unusual experimental structure of $Cp_2ZrCl(CH_2PPh_2)$ (**1**). Various factors influencing monodentate (η^1) vs. bidentate (η^2) ligand coordination of a phosphinomethyl ligand in zirconocene derivatives are analyzed, allowing to extrapolate to other $Cp_2M(X)(A\frown B)$ systems ($A\frown B$: potentially mono- or bidentate ligand) in general. Structural and chemical consequences of one electron reduction of **1** are interpreted on the basis of the MO calculations. $Cp_2ZrCl(CH_2-PPh_2)^{\cdot}$ (d^1) is shown to possess an η^1-phosphinomethyl ligand and to be unstable towards heterolytic loss of Cl^- or $CH_2-PPh_2^-$. The ground state structure of d^1-$Cp_2Zr(CH_2PPh_2)$ is calculated to contain an η^2-phosphinomethyl group, consistent with the observed ESR spectrum of the reduction product of **1**.

Phosphinomethyl-Komplexe des Zirconiums: Eine MO-Studie über Struktur-, Bindungs- und Reaktivitätsprobleme

Die Elektronenstruktur und Geometrie gewinkelter Phosphinomethyl-Sandwichkomplexe von Zr^{IV} und Zr^{III} wird mit Hilfe von Molekülorbital-Berechnungen untersucht. Fragmentorbital-Betrachtungen und störungstheoretische Argumente werden verwandt, um die ungewöhnliche experimentelle Struktur von $Cp_2ZrCl(CH_2PPh_2)$ (**1**) zu erklären. Der Einfluß verschiedener Faktoren auf einzähnige (η^1) gegenüber zweizähniger (η^2) Koordination eines Phosphinomethyl-Liganden in Zirconocenderivaten wird analysiert, eine verallgemeinernde Extrapolation auf andere $Cp_2M(X)(A\frown B)$-Systeme ($A\frown B$: potentiell ein- oder zweizähniger Ligand) ist möglich. Strukturelle und chemische Konsequenzen der Ein-Elektronen-Reduktion von **1** werden auf der Basis von MO-Berechnungen interpretiert. $Cp_2ZrCl(CH_2PPh_2)^{\cdot}$ (d^1) besitzt demnach einen η^1-Phosphinomethylliganden und erweist sich als instabil gegenüber heterolytischer Abspaltung von Cl^- oder $CH_2PPh_2^-$. Die Berechnungen ergeben für die Grundzustandsstruktur von $Cp_2Zr(CH_2PPh_2)$ η^2-Koordination der Phosphinomethylgruppe, diese Struktur ist konsistent mit dem beobachtbaren ESR-Spektrum des Reduktionsproduktes von **1**.

Theoretical understanding of different ligand coordination modes in transition metal complexes plays an important role in organometallic chemistry and is a basic prerequisite for both structural and reactivity concepts. In the course of studies directed towards the synthesis of zirconocene derivatives possessing indirect metal metal

0009–2940/82/0606–2153 $ 02.50/0

linkages and independent ligand sites, *Schore* and *Hope* recently reported[2] the preparation and X-ray crystal structure determination of $Cp_2ZrCl(CH_2PPh_2)$ (**1**, Cp = η^5-C_5H_5). The structure of **1** displays a rather unexpected and unusual feature: despite the electron deficient Zr center (d^0, 16 valence electrons) the phosphorus atom is avoiding donation of its lonepair to the metal to such an extent, that the Zr – C – P angle opens up to 130°, which seems to indicate repulsive interactions between Zr and P.

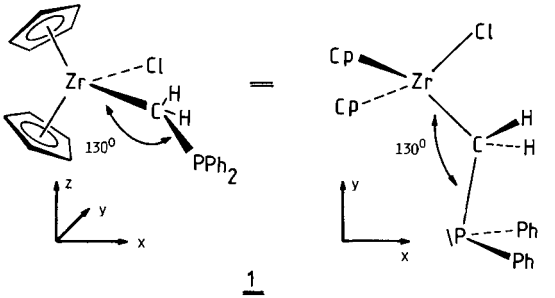

1

As shown in **1**, the PPh_2 unit is located *trans* to the chlorine ligand, the phosphorus atom lying in the $Cl-Zr-C_{CH_2}$ plane.

The observed structure is striking in comparison to other well known phosphinomethyl complexes of metal fragments ML_n with demand for 4-electron ligands. Some typical examples are **2** – **4** or isoelectronic cases like **5** – **7** with aminomethyl or thiomethyl ligands, all bound in a normal η^2-fashion, i.e. as bidentate ligands towards ML_n[3-8].

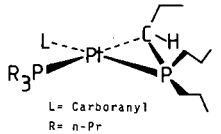

2

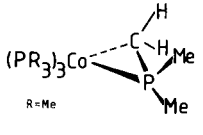

3

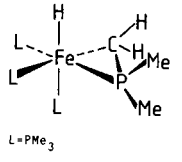

4

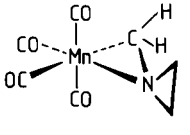

5

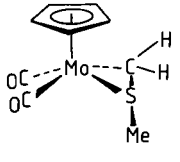

6

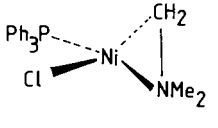

7

Furthermore there exists an increasing amount of structural information, especially from *Floriani's* work[9] revealing acyl ligands, CRO^-, bound via carbon and oxygen in an η^2-fashion in Zr and Ti compounds like **8** – **10**.

Here the observed rearrangement[10] of kinetically controlled primary products **9** formed in CO insertion reactions of $Cp_2Zr(R)_2$ species to the more stable isomers **10** and the reverse acyl coordination in analogous Th derivatives[11] presents an interesting problem in itself and will be treated in detail elsewhere[12].

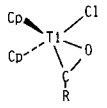

8

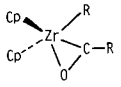

9

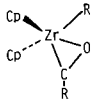

10

8 – 10 are exactly analogous to **1** as far as the metal fragment goes; why then does **1** not only retain its "open shell" metal center, but in addition pushes the P atom away from it?

The observed chemistry of **1** brings up further interesting questions. **1** is easily reduced to some radical anion or radical species (d^1) by Na/Hg, according to scheme 1[13]:

SCHEME 1

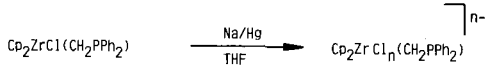

1 n = 0 or 1

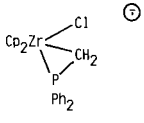

11

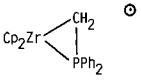

12

The reduced species in solution for several hours shows an intense ESR signal, split by interaction of the d^1 electron with one Zr nucleus ($a(^{91}Zr)$ = 13.5 G) and one P nucleus ($a(^{31}P)$ = 19.5 G). In comparison to known d^1-Zr systems with full Zr – P covalent bonds, this seems to indicate that one-electron-reduction of **1** induces direct Zr^{III} – P interaction which is clearly not present in the neutral precursor. Two alternative η^2-structures were suggested, **11** or **12**, but no decision was possible on the basis of available experimental evidence due to the elusiveness of the reduction product[14].

Prompted by these findings we report here a molecular orbital study, analyzing the ground state electronic structure of **1**, as well as possible coordination alternatives of the phosphinomethyl ligand. Effects on geometry and ligand coordination of adding an electron to **1** are studied. Extended Hückel calculations will be used, augmented by perturbation and symmetry arguments to provide a detailed understanding of the electronic structure of **1** and of its chemistry.

Cp_2ZrCl^+ and $CH_2PH_2^-$ Fragments

A convenient starting point of our analysis of $Cp_2ZrCl(CH_2PPh_2)$, which for the sake of computational simplicity will be first modelled by $Cp_2ZrCl(CH_2PH_2)$, is the valence orbitals of a Cp_2ZrCl^+ unit, **13**, with γ set at an angle as found in many available Cp_2ZrLL' structures[15] and in **1**.

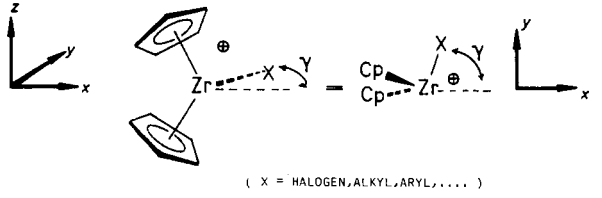

13

This "pyramidal" 14-electron fragment (d^0) then will allow us to construct the molecular orbitals of the complexes and to describe the possible bonding situations for the phosphinomethyl ligand as borne out by the calculations. The orbitals of a Cp_2ZrCl^+ fragment can be easily traced back to the familiar valence MOs of a bent Cp_2M moiety, as described in detail in the literature[16]. It is necessary to decipher the orbitals of **13** with respect to their shape (spatial extent, symmetry) and their energy before we use them to understand the bonding in **1**. Figure 1 shows how the three lowest unoccupied molecular orbitals of Cp_2Zr^{2+}, (d^0, C_{2v}), $1a_1$ (mainly of y^2-character[17]), $b_2(xy, y)$ and $2a_1$ (a mixture of s, x, $x^2 - y^2$ and z^2) interact with the filled p-AOs[18] of Cl^- within the xy-plane (p_σ, p_π).

Extensive mixing among all orbitals shown occurs, caused by the low symmetry. $1a_1$ is destabilized mainly by p_π, the resulting antibonding combination mixes into itself b_2 character (and a small $2a_1$ contribution) as shown in **14** (within the xy-plane):

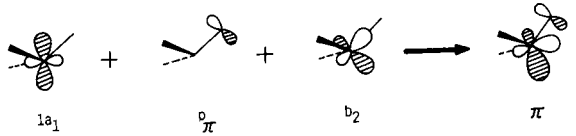

14

15

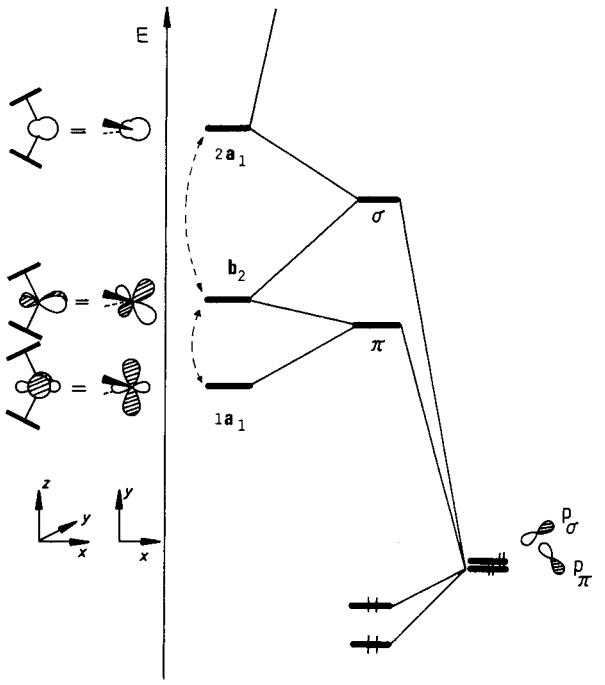

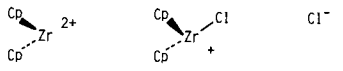

(13)

Figure 1. Valence orbitals of a d^0-Cp_2ZrCl^+ fragment

The orbital decomposed in **14** is the LUMO of Cp_2ZrCl^+. It exhibits π-type character towards the site of a second ligand in the *xy*-plane, and for simplicity will be called π in our context. Its two lobes point approximately along the *x*- and *y*-axis of our coordinate system and are of different size, as clearly revealed by the corresponding plot of the wavefunction[19] in figure 2. This "asymmetry" will turn out to be of some importance[20].

b_2 of Cp_2Zr^{2+} is destabilized by interaction with p_σ (and to a lesser extent with p_π), the resulting MO carries a small antibonding component from $1a_1$ and in addition strongly mixes into itself $2a_1$ in a bonding way with respect to the Cl^- ligand. The composition of this MO is schematically given in **15**.

This orbital, also plotted in figure 2, represents the second low energy acceptor level of Cp_2ZrCl^+; it also is rehybridized nicely towards the vacant ligand position and displays σ character as indicated in **15**. So we will name this valence MO σ.

$2a_1$ of Cp_2Zr^{2+} is so strongly destabilized by the chlorine donor, that it disappears out of the energy range of figure 1. A more formalistic way of describing the orbital

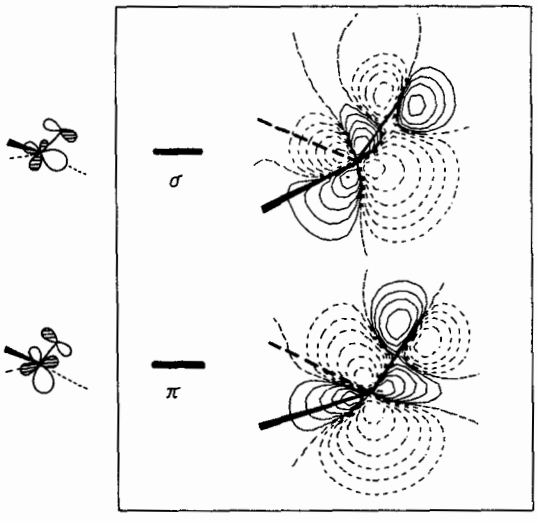

Figure 2. Contour plots for valence MOs σ and π of Cp_2ZrCl^+

interaction finally leading to σ and π could make use of perturbation theory[21] to analyze interfragment polarization within the Cp_2Zr^{2+} orbital manifold, induced by the Cl^- ligand. In any case we are left with a rather simple picture of Cp_2ZrCl^+: the fragment possesses two low lying acceptor MOs, σ and π, suitable for binding additional groups within the *xy*-plane. Cp_2ZrCl^+ thus is ready for establishing bonds to either 2 two-electron or to 1 four-electron donor if the Zr valence shell is to be filled[22]. It should be emphasized, that energy as well as the actual degree of hybridization of σ and π will depend on the electronic nature of X in a Cp_2MX fragment and also upon M and the geometry. This dependence will be addressed at the appropriate point of this paper.

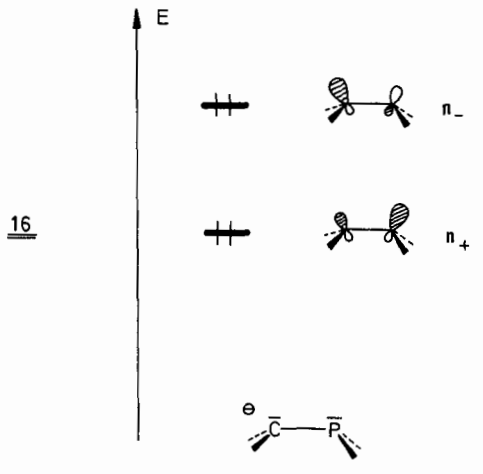

Before we can discuss the ground state structure of $Cp_2ZrCl(CH_2PH_2)$ we must slightly digress to characterize the $CH_2PH_2^-$ ligand, the geometry for the moment being cisoid (lonepairs eclipsed) as in **16**, close to the CH_2PPh_2 conformation in compound **1**.

Two high lying orbitals, n_- and n_+, both filled, have to be considered: the antibonding and bonding linear combination of the carbanion and the P lonepair. n_- is predominantly localized at the carbanionic center, n_+ has its higher density at phosphorus. The relationship of n_- and n_+ to π and π^* of ethylene is obvious.

The splitting of n_- and n_+ as well as their different localization on both ends, in an EH calculation of course will depend on the specific parameters used (H_{ii}-values, basis functions) and the geometry. We will employ standard values but we note already here that the general conclusions of this paper do not change critically with this choice. Furthermore, the picture evolving from EH calculations on $CH_2PH_2^-$ is substantiated (rotational barrier, n_+/n_- splitting, localization) by recent *ab initio* calculations[23], using a split valence basis with diffuse functions added at carbon and phosphorus. Substituents at C and P will play an additional role; we will refer back to this later.

Having delineated a picture of the electronic structure of both the Cp_2ZrCl^+ and the $CH_2PH_2^-$ fragments, we now turn to the complex.

$Cp_2ZrCl(CH_2PH_2)$, Electronic Structure and Ground State Geometry

Our MO calculations first focus on the ground state structure of the model system $Cp_2ZrCl(CH_2PH_2)$. It is obvious that a complete geometry optimization for this molecule is a prohibitive task. But as we are primarily interested in the coordination of the phosphinomethyl ligand, the Cp_2Zr part of all systems studied has been kept fixed with a geometry adapted from **1** and related compounds. Then the variable spatial arrangement of the two ligands in question, Cl^- and $CH_2PH_2^-$, can be defined best by three angular parameters, α, β, γ, shown in **17**, the η^1-structure of $Cp_2ZrCl(CH_2PH_2)$. These angles determine the position of both groups in the *xy*-plane for given distances Zr – Cl, Zr – C, and C – P.

Note that β corresponds directly to the intrigueing Zr – C – P angle of **1** and that coordination of the P lonepair to the metal would mean a small β (and accordingly changed α and γ values).

A number of geometry optimizations has been performed first within the (α, β, γ)-space, thereby retaining a plane of symmetry (the *xy*-plane) throughout. Four basically different conformations for an in-plane monodentate $CH_2PH_2^-$ fragment (η^1-bound via carbon) are possible here.

17, as found for **1**, has its C – P bond *trans* to the Zr – Cl bond, the phosphorus lonepair is *cis* to the Zr – C bond. Alternatively, **18**, **19**, and **20** are C_s-rotamers with respect to the Zr – C and the C – P bonds.

Let us use the notation η^1(*trans/cis*) for **17**, η^1(*trans/trans*) for **18**, η^1(*cis/cis*) and η^1(*cis/trans*) for **19** and **20**. Varying α, β, and γ in the case of **17** and **19** should allow a transformation to the corresponding η^2-structures η^2(*trans*), **21**, and η^2(*cis*), **27**, respectively, if such minima do exist[24]. All η^1-species **17** – **20** and geometries in between are interconnected by two additional degrees of freedom, namely rotations around the Zr – C and the C – P linkages. The variation of these parameters has also been tested in model calculations.

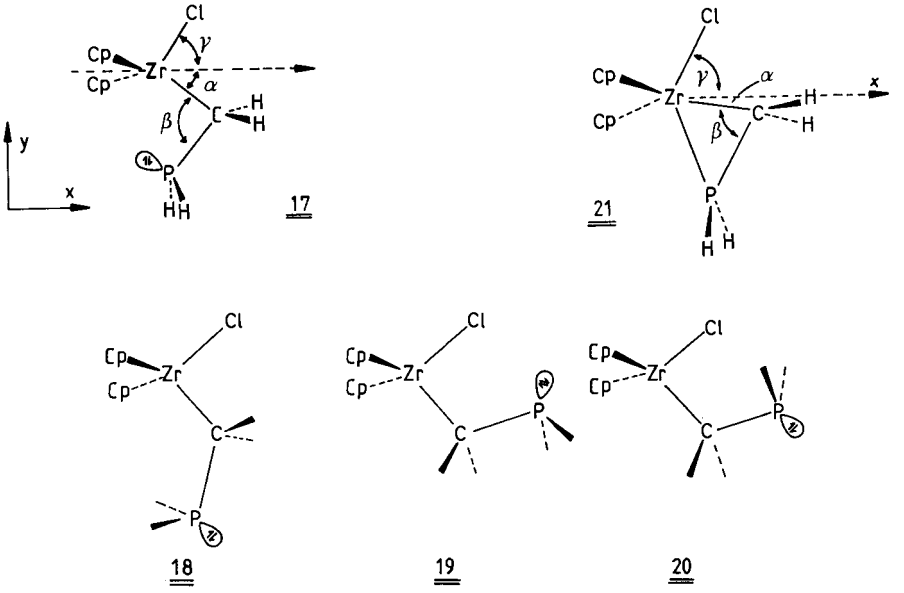

Let us start our electronic analysis from **17**, η^1(*trans/cis*). A complete geometry search interestingly leads to *two* distinct minima on the (α, β, γ) energy surface. One minimum structure is indeed **17**, $\alpha = 45°$, $\beta = 140°$, $\gamma = 45°$. This yields a Cl – Zr – C angle of 90° (experimentally 90.4° for **1**) and a Zr – P distance of 3.88 Å (3.76 Å experimental value in **1**). The structure closely resembles the X-ray geometry of **1** and, most

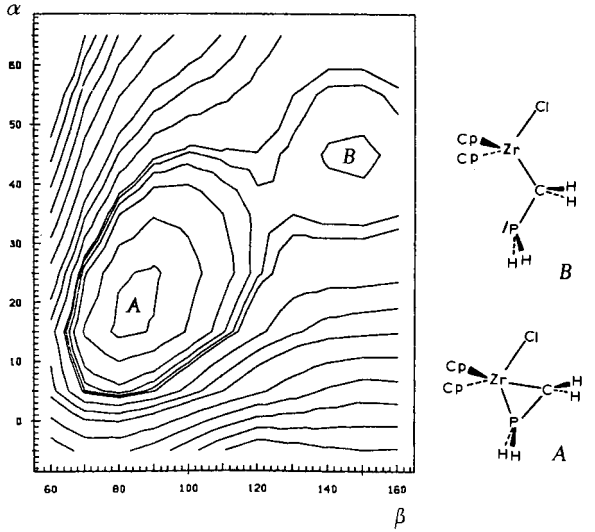

Figure 3. Energy contour map for $Cp_2ZrCl(CH_2PH_2)$, optimizing α and β at a fixed value of $\gamma = 55°$. The contour lines are not equidistant, for absolute values see text. The coordination of the $CH_2PH_2^-$ ligand is as in **17**

importantly, does in fact reproduce the unusually wide Zr – C – P angle, which comes out somewhat larger than in the real compound and which we need to understand. The second minimum found by the calculation is clearly a η^2-structure as shown in **21**, derived from η^1(*trans/cis*) **17** by attaching the phosphorus donor to the metal and filling up the Zr valence shell. Here we find $\alpha = 15°$, $\beta = 80°$ and $\gamma = 65°$, giving a Zr – P distance of 2.67 Å, which represents a fully developed bond. The geometry of **21** is comparable to other stable 18-electron $CpML_3$ systems[25] and in particular to the aforementioned acyl structures[9].

The η^2-minimum in the calculations of the model $Cp_2ZrCl(CH_2PH_2)$ is of *lower* energy than the η^1-structure, actually by some 28 kcal/mole. Interconverting **17** ⇌ **21**, described by the appropriate changes in α and β, is accompanied by a change in γ of about 20°. Although we cannot present a simple graphic representation for the minimum energy pathway $\eta^1 \rightleftharpoons \eta^2$ in all three degrees of freedom we can do so for an intermediate value of γ, keeping this variable fixed, and this is done in the energy contour diagram of figure 3.

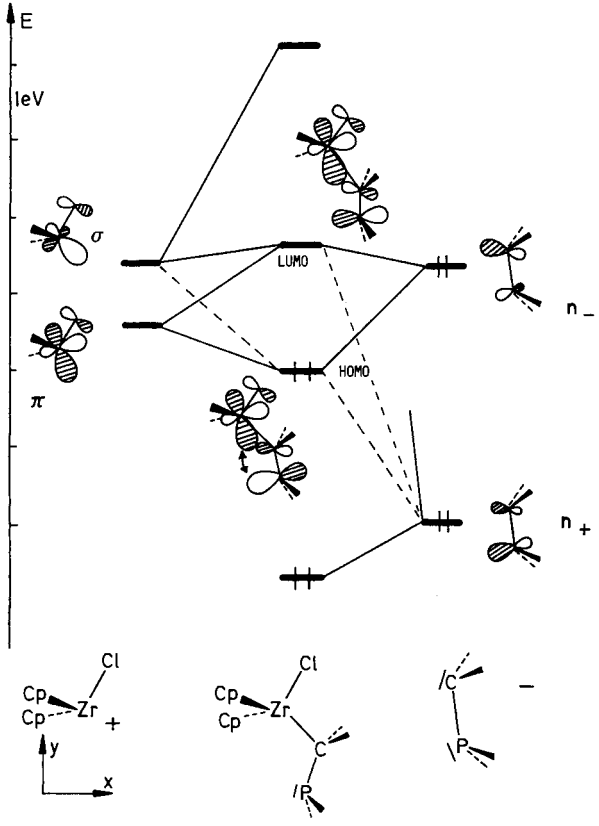

Figure 4. Simplified interaction diagram of Cp_2ZrCl^+ with $CH_2PH_2^-$ for the η^1-geometry **17**

The two minima marked A (η^2) and B (η^1) here of course differ from the absolute minima described above, as neither one allows for a full relaxation of all three angles. But as can be seen, both are separated by an energy barrier. At first glance it seems rather disappointing, that our calculations predict an η^2-bonding mode of the phosphinomethyl ligand $CH_2PH_2^-$, in contrast to the experimental structure of the diphenyl compound **1**. Actually the energy ordering, η^1 vs. η^2, turns out not to be a very relevant point in our analysis. A closer inspection of the electronic situation will reveal a series of factors influencing the relative preference for either ligand attachement and we will turn back to this soon.

Of crucial significance, however, are the findings that two different minima are possible for $Cp_2ZrCl(CH_2PH_2)$, that their interconversion has to overcome an energy barrier and that the calculated η^1(*trans/cis*) isomer **17** reproduces the essential features from the experimental structure determination of **1**.

To explain these results we may start from figure 4. It represents a simplified interaction diagram between Cp_2ZrCl^+ and $CH_2PH_2^-$ valence MOs as described previously. All the orbitals shown, σ, π, n_-, and n_+ belong to the same symmetry; they all interact, but it is easy to single out the most dominant contributions to each of the four resulting frontier orbitals of the complex, and only those are shown.

The η^1-bound $CH_2PH_2^-$ ligand causes strong interaction of n_+ and n_- with σ of Cp_2ZrCl^+. One resulting level is sent to high energy, while n_+ ends up in a stabilized MO (the lowest one in figure 4), which carries a large part of the Zr – C bonding. Of much more interest in our context are the two remaining molecular orbitals of $Cp_2ZrCl(CH_2PH_2)$, the HOMO and the LUMO of the η^1-complex. Their main contribution comes from n_- and π, both close in energy and of appreciable overlap for this geometry. The HOMO is the bonding combination of π and n_-, kept from being stabilized much by an admixture of n_+, in an antibonding way towards π. This 3-level mixing pattern for the HOMO is depicted in **22**:

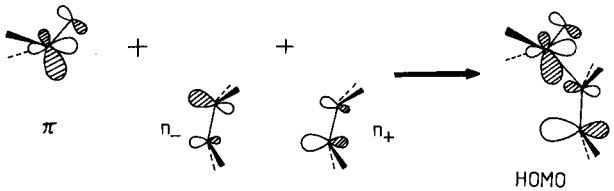

22

A contour plot of the HOMO is given in figure 5b. The orbital is Zr – Cl antibonding, Zr – C bonding and, most significant, Zr – P antibonding. The mixing with n_+, as in **22**, leads to increased localization of the wavefunction on phosphorus and to a decrease of the carbon contribution. So for the η^1(*trans/cis*) configuration of the complex the HOMO takes over part of the Zr – C bond and, predominantly, lonepair character at P. Note that the Zr – C bonding in this high lying occuppied MO necessarily causes strong Zr – P antibonding interaction. This is the electronic reason, why compound **1** (and our model $Cp_2ZrCl(CH_2PH_2)$ as well) inevitably couples η^1(*trans/cis*) coordination of the phosphinomethyl ligand to an abnormally large

Zr – C – P angle, thus reducing Zr – P repulsion and lowering the energy of the HOMO. If our picture is correct, the Zr – P repulsion must also show up in the calculated reduced overlap populations. Indeed n_{Zr-P} comes out as -0.10 for the minimum structure **17**.

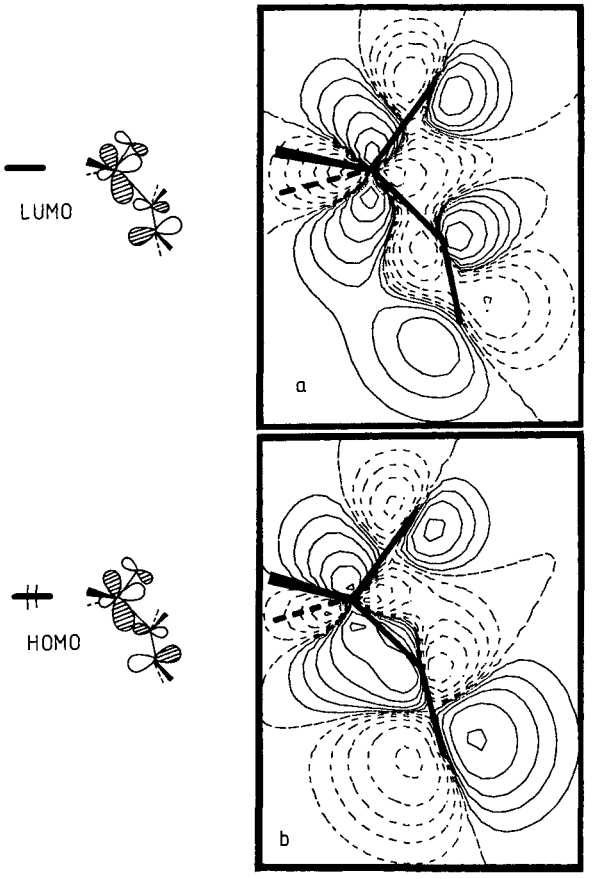

Figure 5. Contour maps of HOMO and LUMO of $Cp_2ZrCl(CH_2PH_2)$ for η^1-minimum structure η^1 (*trans/cis*), **17**

The LUMO in figure 4 results from the antibonding combination of π with n_-, this MO mixes in some amount of σ of Cp_2ZrCl^+. It is separated by some 1.7 eV from the HOMO. This gap within the extended Hückel formalism assures a singlet ground state, but in passing we note that the LUMO is rather low in energy, which should make reduction of the system easy. Figure 5a gives a contour plot of the LUMO; it is Zr – Cl antibonding, Zr – C antibonding and Zr – P bonding.

The nodal character of the LUMO will be important if we discuss the reduction chemistry of **1**. Remember that reduced **1** displays strong phosphorus coupling in its ESR spectrum, which might be indicative of direct Zr – P interaction induced by populating the LUMO.

Now we can turn to the η^2(*trans*) minimum structure of $Cp_2ZrCl(CH_2PH_2)$ and to an analysis of possible $\eta^1 \rightleftharpoons \eta^2$ interconversions. Figure 6 is a truncated interaction diagram for the computed η^2(*trans*) geometry **21** of our model. Here, in contrast to the previous case of **17**, the nodal properties of both frontier levels π and n_- match perfectly. Both termini end up bonding to the two lobes of π in the HOMO of the complex. The HOMO here is lower in energy, the π/n_- antibonding combination is much higher than that for **17**. It is not the LUMO any more, but the LUMO of structure **21** is the *xz*-fragment orbital of Cp_2ZrCl^+, derived from b_1 of a bent Cp_2M moiety[16,26]. σ of Cp_2ZrCl^+ is again pushed up, out of the picture of figure 6, n_+ is stabilized by interacting both with σ (more) and π (less). Figure 7 sketches a contour map of the η^2-HOMO, (note its resemblance to one of the Walsh MOs of cyclopropane[27]) and its bonding character between Zr and C as well as Zr and P. It is very instructive now to take a look at the energy variation of the HOMO and the LUMO which accompanies an $\eta^1 \rightleftharpoons \eta^2$ interconversion. For simplicity we have drawn this Walsh type diagram in figure 8 for the approximate minimum energy pathway $\eta^1 \rightleftharpoons \eta^2$ (B $\rightleftharpoons$ A) on the energy surface of figure 3; that is keeping γ fixed at 55°, varying α and β together[28].

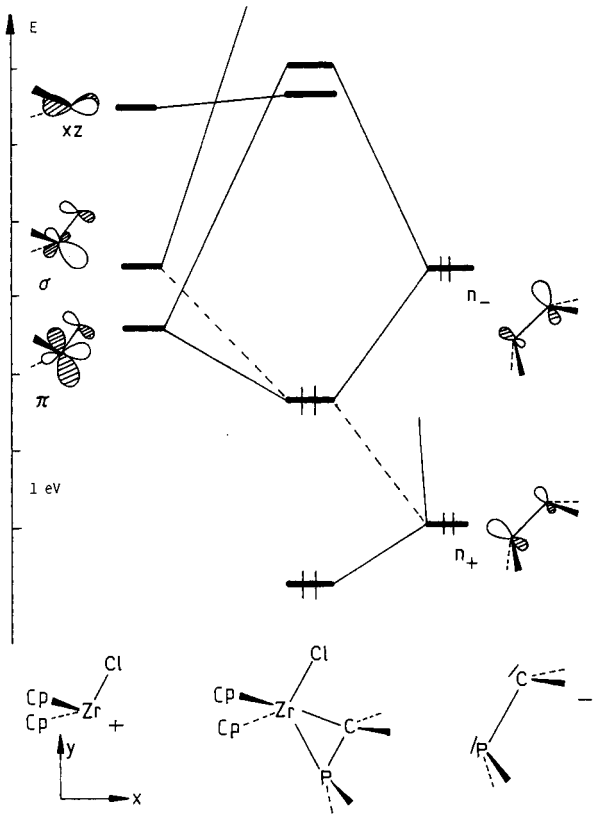

Figure 6. Simplified interaction diagram of Cp_2ZrCl^+ and $CH_2PH_2^-$ MOs for η^2-minimum structure η^2(*trans*), **21**

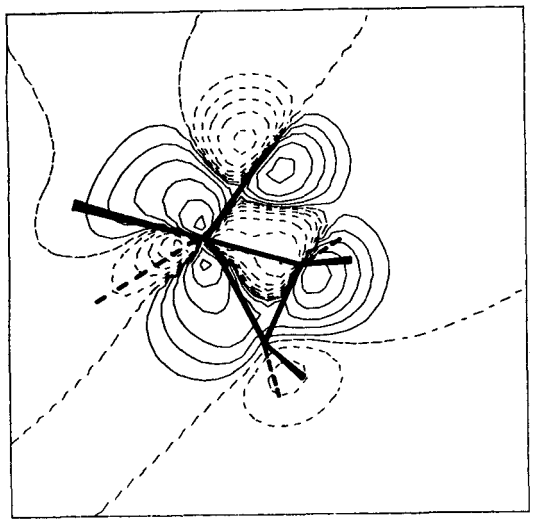

Figure 7. Contour plot of the HOMO of $Cp_2ZrCl(CH_2PH_2)$, η^2(*trans*), **21**

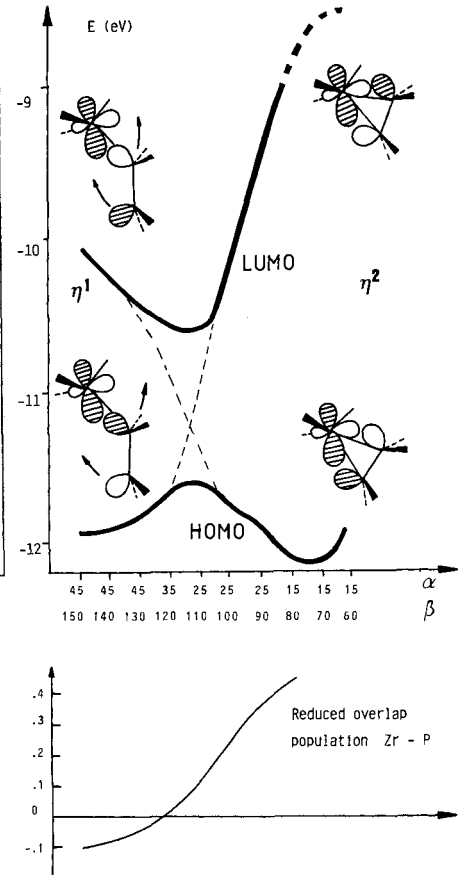

Figure 8. HOMO/LUMO Walsh diagram for η^1(*trans/cis*) $\rightleftharpoons$ η^2(*trans*) interconversion (**17** $\rightleftharpoons$ **21**), along the approximate minimum energy pathway of energy contour diagram of fig. 3. The lower-part of the figure shows the Zr – P reduced overlap population and its variation along the same-angular coordinates. The broken line for the LUMO at right indicates that *xz* is lower in energy-here (see text)

The geometrical changes, indicated by arrows in figure 8, cause an interesting behavior of the two frontier levels. The HOMO, starting from η^1, gets destabilized first, passes an energy maximum and finally, for η^2, becomes more stable than it was for η^1. In contrast, the LUMO comes down first and, after the transition point, is very strongly destabilized, so that at the very right hand side of the diagram it is not even the LUMO any more. These energy level shifts can be easily understood from overlap changes due to the nodal properties of the MOs involved and indicated schematically in figure 8. The geometry change in a sense causes an avoided HOMO-LUMO crossing, leading to the observed barrier between both structures and isolating them on the energy surface as two distinct minima. By rearranging the $CH_2PH_2^-$ fragment along the $\eta^1 \rightleftharpoons \eta^2$ coordinate, the η^1-HOMO intends to correlate to the η^2-π/n_- antibonding unoccuppied MO. The Zr – P interaction, as expressed by the reduced overlap population

n_{Zr-P}, with its negative value for **17**, changes to strong bonding (η^2: +0.46), passing through zero at the point of minimal HOMO-LUMO separation.

So far we have been focussing on the structure of $Cp_2ZrCl(CH_2PH_2)$ for a specific ligand arrangement as in **17** and, ultimately, **21**. Some questions immediately come to mind from our analysis. Why, for instance, does neither structure **18**, η^1(*trans/trans*), nor any other rotational orientation of the pyramidal PH_2 group (i.e. of the P lonepair) result in a lower computed energy than found for **17**? Given the structure determining Zr – P repulsion, located within the HOMO of **17**, it would seem natural that the molecule escapes from such a situation by rotating the offending lonepair out of the Cl – Zr – C plane, or by putting it *trans* to the Zr – C bond as in **18**. This could bring back the Zr – C – P angle to a normal sp^3-angle. While for the "real" diphenylphosphinomethyl system **1** one might easily argue that **17** is preferred for steric reasons, this point of course does not hold for our model with a PH_2 group, where η^1-geometries do not get sterically hindered. The answer is found in the $CH_2PH_2^-$ ligand itself. In **18**, this fragment has *trans* oriented lonepairs at C and P. Consequently the ligand HOMO n_-, mainly responsible for the antibonding Zr – P interaction in the HOMO of the complex, is different from n_- of a cisoid (eclipsed) $CH_2PH_2^-$ as bound to Cp_2ZrCl^+ in **17**. For **18** the n_- orbital is seen in **23**, as opposed to n_- in **16**.

So for **18** the interaction with n_- leads to even stronger Zr...P antibonding via the back lobe of the phosphorus lonepair, directed towards zirconium. This could be documented by the contour plot of the HOMO of **18** compared to that of the HOMO of **17** (figure 5b); the qualitative difference between both cases is shown in **24** and **25**.

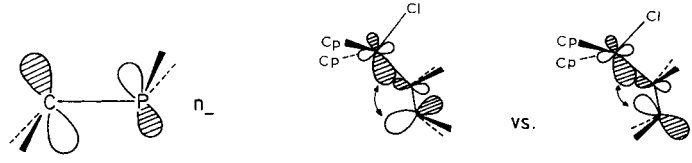

23 **24** **25**

It still remains to explain why *gauche*-type conformations like **26** (P lonepair of **17** or **18** twisted out of, or perpendicular to, the Cl – Zr – C plane) are also less stable than **17**.

The reason lies in the energy split between n_- and n_+ of $CH_2PH_2^-$. Figure 9 gives a qualitative picture of the conformational dependence of the n_-/n_+ energy level splitting – a familiar situation for any bond-twisted π-system. **26** would correspond to a ligand geometry with strongly reduced n_+/n_- energy separation and a low lying n_- orbital. Consequently a reduction of Zr – P antibonding by out of plane rotation around the C – P bond has to be payed for with a weaker Zr – C bond, as n_- moves to lower energy and – as a weaker σ-donor – interacts less with the Cp_2ZrCl^+ acceptor MOs. The calculations on our model $Cp_2ZrCl(CH_2PH_2)$ show that it prefers to keep optimal Zr – C bonding to the cost of some Zr – P repulsion and Zr – C – P angle opening, the latter being minimal for η^1(*trans/cis*), **17**, close to the real structure. Rotation around the Zr – C bond is possible only for η^1-structures, ligand rotation of a

η^2-bound $CH_2PH_2^-$ is sterically and electronically inaccessible. But even when the phosphinomethyl ligand is η^1-connected to the metal fragment, the PH_2 or (much more so) the PPh_2 part of the molecule interfers with the Cp rings if it is to move out of the "equatorial" plane by twisting around the Zr – C bond. (Fragment MOs σ and π have their maximum extension in this plane anyway.)

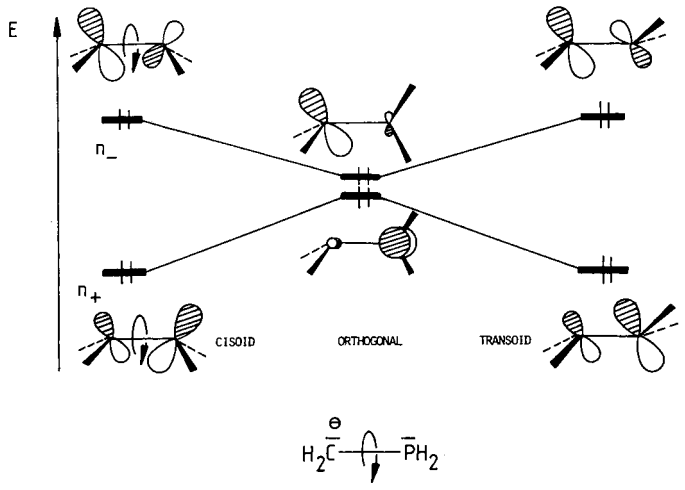

Figure 9. Qualitative representation of the conformational dependence of n_+/n_- splitting for $CH_2PH_2^-$

Interestingly the calculations do not lead to an η^1(*cis/cis*) or η^1(*cis/trans*) local minimum **19** or **20** on the (α, β, γ) surface. Only one other stable ligand arrangement is found, namely the η^2-isomer, η^2(*cis*), **27**, derived from **19**.

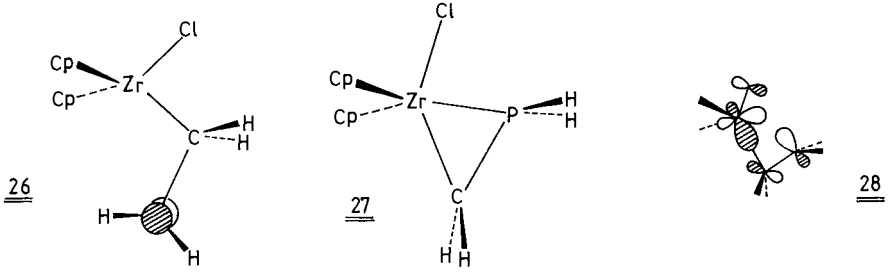

Its energy in the calculations is practically identical to that of the other η^2-geometry **21**. A corresponding η^1-structure **19** collapses to this species without any barrier, if an energy surface like the one of figure 3 is computed. The HOMO for an intermediate η^1 waypoint is represented in **28**. Here the phosphorus lonepair contribution is directed towards the nodal plane of π, with even some positive overlap to its smaller lobe. An η^1-situation thus does not suffer from a strong Zr – P antibond. The conversion to η^2 here proceeds smoothly without a noticeable barrier, no η^1-minimum exists.

So in summary we are left with three minimum structures for $Cp_2ZrCl(CH_2PH_2)$, **17**, **21** and **27**, whose bonding situations we have unravelled in detail.

Factors Determining the η^1/η^2 Energy Difference

At this point it is necessary to come back to the computed energy ordering of these three isomers of our model. Remember that both η^2-structures are ca. 28 kcal/mole more stable in the calculations than the η^1-geometry that corresponds to the X-ray structure of **1**. Also the calculated barrier between **17** and **21** is rather small, roughly 5 – 6 kcal/mole. Although we think that these numbers are not important for understanding the basic bonding situation, we have to analyze those factors which will play a role in determining the energy ordering of η^1 vs. η^2 in general. We will do so by comparing the structurally coupled η^1 and η^2 isomers **17** and **21** with respect to their energy difference as a function of steric and electronic influences.

In order to see the effect caused by modelling the PPh_2 group by PH_2, some calculations for $Cp_2ZrCl(CH_2PPh_2)$ (**1**) were also performed. The η^2-structure **21** here inevitably runs into steric trouble, of course much more so than the η^1-alternative **17**. In fact the η^2-preference is reduced by some 23 kcal to about 5 kcal! This is certainly an important point in compound **1**, though electronically not so interesting.

Decisive significance, however, in determining the η^1 vs. η^2 coordination mode in an electronic sense has to be attributed to the following factors in a general $Cp_2MX(\widehat{A}B)$ system, ($X = Cl^-$ and $\widehat{A}B = CH_2PH_2^-$ in our case):

a) The choice of the metal parameters (this corresponds to a change of the metal M, if we want to extrapolate to other related compounds).

b) The choice of the phosphorus parameters (for instance modelling substituent effects at P or a replacement of P by a different lonepair carrying group).

c) The effect of the additional ligand X.

All our calculations for $Cp_2ZrCl(CH_2PH_2)$ have made use of the metal parameters given in the appendix, the Zr valence state ionization potentials taken somewhat arbitrarily from earlier work on Nb compounds as approximate values. When we perform a self-consistent-charge iterative calculation[29] on the experimental geometry of **1** to get more realistic H_{ii} values for Zr, the metal 4d ionization potential at convergence is about 1 eV lower (– 11.2) than the one we had used in our model calculations. A consequence of a less electronegative metal center, of course is a higher lying Cp_2ZrCl^+ MO π in figure 1 and, accordingly, a smaller preference for η^2-bonding of the phosphinomethyl ligand. Using those more realistic SCC parameters for Zr reduces the η^2-energy advantage for $Cp_2ZrCl(CH_2PH_2)$ by 10 – 11 kcal. We note that adding the effect of the sterically encumbering PPh_2 instead of PH_2 and of improving the Zr H_{ii}'s already suffice to make **17**, the η^1-structure, *more stable.* The general description of bonding is not altered by the variation in the parameters employed and we did not consider it worthwhile to improve the numerical details of this study. The analysis of effects caused by replacement of P by a better or worse donor we leave to the reader. The change of X in $Cp_2MX(\widehat{A}B)$ molecules with monodentate or bidentate bonding option has some interesting experimental background. Remember that the LUMO of Cp_2ZrCl^+, π, is destabilized by Zr – Cl π-antibonding interactions (cf. figure 1). Re-

placing the π-donor Cl^- by say H^- or $alkyl^-$ of pure σ donating capability will, therefore, keep π at lower energy, more accessible as an acceptor level. This should lead to an increased stabilization for η^2, bidentate coordination of additional ligands A⌒B. Without going into details here[30] we would like to mention that **29** is fluxional[31] while **30** isn't, confirming our picture.

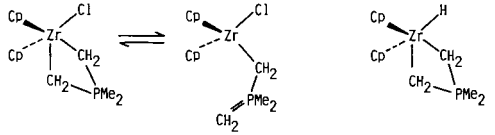

29 **30**

The Reduced d^1-Species

We are ready now to address reactivity questions posed by *Schore*'s observations in the course of reduction experiments performed with **1**. In particular the structure of the ESR observable d^1-species with pronounced coupling to the Zr and P nuclei, suggesting **11** or **12**, is of interest. Adding an electron to $Cp_2ZrCl(CH_2PPh_2)$ (**1**) or $Cp_2ZrCl(CH_2PH_2)$, η^1(*trans/cis*), **17** as a model, populates the low lying LUMO. We im-

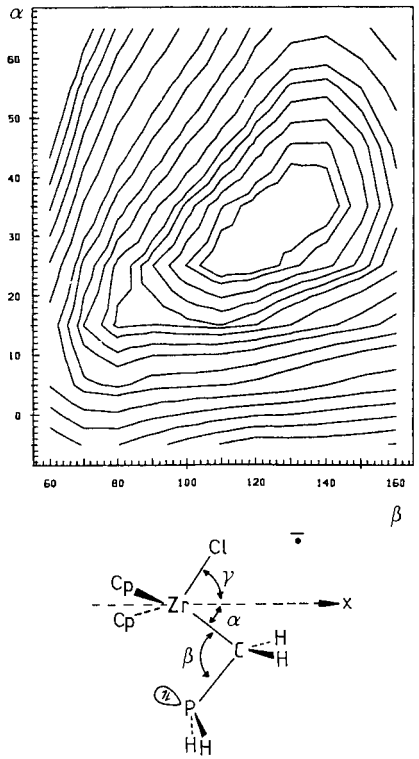

Figure 10. $\eta^1 \rightleftharpoons \eta^2$ energy contour map for radical anion $Cp_2ZrCl(CH_2PH_2)^-$

mediately can tell about the direction of geometry relaxation caused by the reduction step. As apparent from the $\eta^1 \rightleftharpoons \eta^2$ Walsh diagram of figure 8, the former LUMO, now singly occuppied, Zr – C antibonding and Zr – P bonding, will be stabilized if the $CH_2PH_2^-$ ligand relaxes somewhat towards a η^2 situation, reducing Zr – C repulsion and strengthening the Zr – P bonding interaction. This geometric change will not go very far, however, because on the η^1-side the stabilization due to the half occuppied level is soon exceeded by the energetic ascent of the doubly occuppied MO below (the HOMO of the neutral complex). On the η^2-side of the diagram the singly occuppied orbital is drastically destabilized. The $\eta^1 \rightleftharpoons \eta^2$ energy surface for the radical anion $Cp_2ZrCl(CH_2PH_2)^-$, calculated identically to the surface for its neutral precursor in figure 3, is shown in figure 10 and it manifests our expectation.

Only one minimum with η^1-geometry appears, β is reduced by about 20°, α by about 10° compared to **17**. As our parameters tend to disfavor η^1-structures anyway, we can safely state that no η^2-structure for $\mathbf{1}^-$ like **11** is possible and that the ESR signal does not come from **11**, but has to result from some other species.

Population of the LUMO of the complex, aside from the "slipping" of the $CH_2PH_2^-$ ligand, induces an overall weakening of the Zr – C and the Zr – Cl bonds. Table 1 gives the reduced overlap populations for both η^1-minimum energy structures of $Cp_2ZrCl(CH_2PH_2)$ and its radical anion.

Table 1. Relevant reduced overlap populations for η^1-$Cp_2ZrCl(CH_2PH_2)$ and its radical anion

Reduced overlap population	$Cp_2ZrCl(CH_2PH_2)$ molecule	$Cp_2ZrCl(CH_2PH_2)^-$ radical anion
Zr – Cl	0.624	0.555
$Zr - C_{CH_2}$	0.598	0.537
Zr – P	−0.083	0.074

A plausible consequence of initial 1-electron reduction, therefore, seems to be a heterolytic cleavage of either the zirconium – chlorine or the zirconium – carbon bond, leading irreversibly to a d^1-$Cp_2Zr(CH_2PPh_2)$ radical and Cl^- in the former case. $Cp_2Zr(CH_2PPh_2)$, **12**, then would be the persistent radical species in solution, provided its structure can explain the coupling to the phosphorus in the ESR experiment. Actually a number of compounds, isoelectronic to **12**, all with η^2-bonding $\overset{\frown}{AB}$ ligands, are known. Some examples are **31** – **34**[32–35].

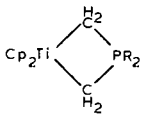

31

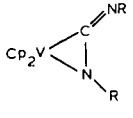

32

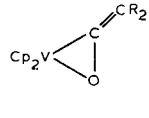

33

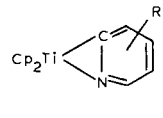

34

If we calculate the minimum energy structure for $Cp_2Zr(CH_2PH_2)$ using the angular variables α and β in **35** we get the contour map of figure 11, with only η^2 coordination available. The Zr – C – P three membered ring has Zr – C = 2.28 Å (fixed), C – P = 1.85 Å (fixed), Zr – P = 2.39 Å, $\alpha = 40°$, $\beta = 70°$, yielding an angle C – P – Zr of 64°.

So we are led to conclude that the species formed from **1** by reduction is **12**. It is impossible to reliably calculate the energy required for Zr – Cl vs. Zr – C bond-breaking, but it seems reasonable to assume that bond strength and also solvation will make Cl^- loss more favorable[36]. **12** contains a full covalent Zr – C and Zr – P bond, the unpaired electron resides in an orbital with preponderant metal (y^2) character, but with additional contributions from C and P in the wavefunction as shown in figure 12. Delocalization of the unpaired electron to the phosphorus, where the MO wavefunction exhibits some amount of s character is consistent with the ESR spectrum.

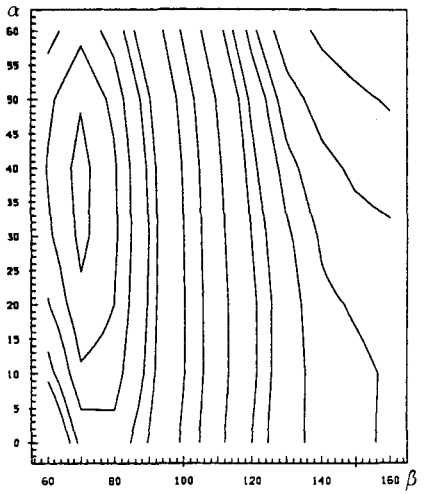

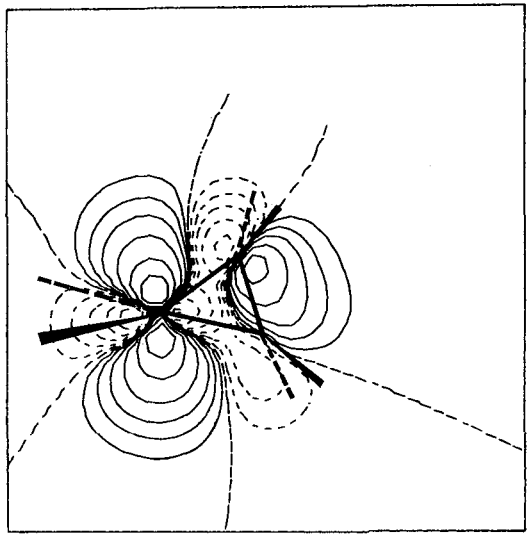

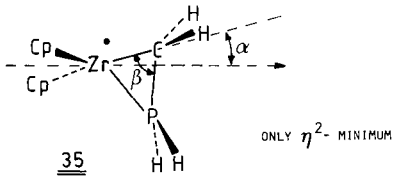

35

Figure 11. Energy surface for optimizing $Cp_2Zr(CH_2PH_2)$, angular variables as in **35**

Figure 12. Contour plot of half-occuppied MO of d^1-$Cp_2Zr(CH_2PH_2)$, corresponding to minimum structure of fig. 11

Concluding Remarks

In this paper we have concentrated on a rather specific organometallic molecule, $Cp_2ZrCl(CH_2PPh_2)$ (**1**), and models thereof, intrigued by its rather unusual solid state structure and by its chemical behaviour upon reduction. Our molecular orbital analysis allows us to understand all the experimental observations and, relying predominantly upon overlap, symmetry and perturbation arguments, it should be method independent. It also makes extrapolation to other related systems of the type $Cp_2MX(A\frown B)$

possible. This class of compounds includes not only the fascinating titanocene and zirconocene acyl complexes mentioned in the introduction, which seem to play a key role in CO insertion and homogeneous CO reduction processes[37], but also systems like **29** or **36**[38] with fluxional character. The $Cp_2MX(A\frown B)$ family of molecules even extends to bimetallic and non-rigid species like **37**[39] (rapid CO exchange between terminal and bridging positions is observed in this case; **37** is a η^2-case in our notation) or **38**[40] (Cp* = η^5-C_5Me_5). The X-ray structure of **38** shows end-on oxygen coordination of the $CpMo(CO)_3^-$ fragment to a Cp_2MX^+ group (a η^1-case), in contrast to **37**.

Certainly the phosphinomethyl ligand will lead to further interesting chemistry in the early transition metal field. We hope to have contributed somewhat to its understanding.

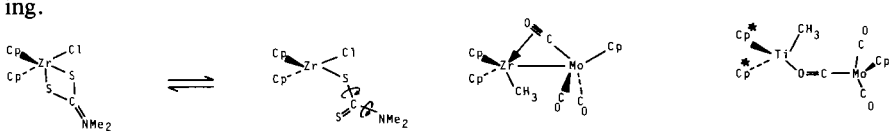

36 **37** **38**

We thank the *Deutsche Forschungsgemeinschaft* and the *Fonds der Chemischen Industrie* for financial support. The cooperation of *the staff of the Regionales Rechenzentrum, Universität Erlangen,* is gratefully acknowledged. We also thank Profs. *R. Hoffmann, P. v. R. Schleyer* and Drs. *K. Tatsumi* and *Odile Eisenstein* for communicating unpublished work. P.H. gratefully acknowledges the hospitality of Prof. *E. O. Fischer* at the Anorganisch-Chemisches Institut der TU München, where this work was written up.

Appendix

All calculations are of the Extended Hückel type[41], with standard parameters for carbon and hydrogen used. The modified Wolfsberg-Helmholz formula[42] was employed throughout. The atomic parameters for Zr[43], Cl[44] and P[43] are given in Table 2.

Table 2. Extended Hückel parameters

	Orbital	H_{ii}(eV)	Exponents[a] ξ_1	ξ_2
Zr	5s	−10.10	1.776	
	5p	−6.86	1.817	
	4d	−12.10	3.835 (.6211)	1.505 (.5796)
Cl	3s	−30.00	2.033	
	3p	−15.00	2.033	
P	3s	−18.60	1.75	
	3p	−14.00	1.30	

[a] Coefficients of the double zeta 4d-functions are given in brackets.

Geometries

Distances were chosen as follows. Cp rings: local D_{5h} symmetry, C−C = 1.4 Å, C−H = 1.08 Å. All $Zr-C_{Cp}$ = 2.5 Å. Zr−Cl = 2.45 Å, $Zr-C_{CH_2}$ = 2.28 Å, C−P = 1.85 Å, C−H of CH_2 = 1.10 Å, P−H = 1.42 Å.

Angles: Cp−Zr−Cp = 130°, H−C−H = 108°, H−P−H and R−P−R of PH_2 and PPh_2 = 109°. Phenyl rings: local D_{6h} symmetry, distances as in Cp rings.

[1] [1a] Universität Erlangen. – [1b] University of California Davis.
[2] *N. E. Schore* and *H. Hope*, J. Am. Chem. Soc. **102**, 4251 (1980).
[3] *N. Bresciani, M. Calligaris, P. Denise, G. Nardin*, and *L. Randaccio*, J. Am. Chem. Soc. **96**, 5442 (1974).
[4] *H. H. Karsch, H.-F. Klein*, and *H. Schmidbaur*, Angew. Chem. **87**, 630 (1975); Angew. Chem., Int. Ed. Engl. **14**, 637 (1975).
[5] *H. H. Karsch*, Chem. Ber. **111**, 1650 (1978).
[6] *E. W. Abel, R. J. Rowley, R. Mason*, and *K. M. Thomas*, J. Chem. Soc., Chem. Commun. **1974**, 72.
[7] *E. R. de Gil* and *L. F. Dahl*, J. Am. Chem. Soc. **91**, 3751 (1969).
[8] *D. Sepelak, C. G. Pierpont, E. K. Barefield, J. T. Budz*, and *C. A. Poffenberger*, J. Am. Chem. Soc. **98**, 6178 (1978).
[9] *G. Fachinetti* and *C. Floriani*, J. Organomet. Chem. **71**, C5 (1974); *G. Fachinetti, C. Floriani*, and *H. Stoeckli-Evans*, J. Chem. Soc., Dalton Trans. **1977**, 2297; *G. Fachinetti, C. Floriani, F. Marchetti*, and *S. Merlino*, J. Chem. Soc., Chem. Commun. **1976**, 522; *G. Fachinetti, G. Fochi*, and *C. Floriani*, J. Chem. Soc., Dalton Trans. **1977**, 1946.
[10] *G. Erker* and *F. Rosenfeldt*, Angew. Chem. **90**, 640 (1978); Angew. Chem., Int. Ed. Engl. **17**, 605 (1978); *G. Erker* and *F. Rosenfeldt*, J. Organomet. Chem. **188**, C1 (1980).
[11] *P. J. Fagan, J. M. Manriquez, T. J. Marks, V. W. Day, S. H. Vollmer*, and *C. S. Day*, J. Am. Chem. Soc. **102**, 5393 (1980); *P. J. Fagan, J. M. Manriquez, S. H. Vollmer, C. S. Day, V. W. Day*, and *T. J. Marks*, ibid. **103**, 2206 (1981).
[12] *R. Hoffmann, P. Hofmann*, and *K. Tatsumi*, in preparation.
[13] A full report on the reduction chemistry of **1** and of related species will appear separately: *N. E. Schore*, unpublished results. For work on irreversible reduction reactions of Cp_2ZrCl(alkyl) systems see also: *M. F. Lappert, C. J. Pickett, P. I. Riley*, and *P. I. W. Yarrow*, J. Chem. Soc., Dalton Trans. **1981**, 805.
[14] The reduced Zr^{III} species is persistent in solution for many hours, but could not be isolated.
[15] *J. Jeffery, M. F. Lappert, N. T. Luong-Thi, J. L. Atwood*, and *W. E. Hunter*, J. Chem. Soc., Chem. Commun. **1978**, 1081; *J. Jeffery, M. F. Lappert, N. T. Luong-Thi, M. Webb, J. L. Atwood*, and *W. E. Hunter*, J. Chem. Soc., Dalton Trans. **1981**, 1593; *Y. Dusausoy, J. Protas, P. Renaut, B. Gautheron*, and *G. Tainturier*, J. Organomet. Chem. **157**, 167 (1978); *C. H. Saldarriaga-Molina, A. Clearfield*, and *I. Bernal*, ibid. **80**, 79 (1974); *I. A. Ronova, N. V. Alekseev, N. I. Gapotchenko*, and *Y. T. Struchkov*, ibid. **25**, 1245 (1969); *J. L. Atwood, C. K. Barker, J. Holton, W. E. Hunter, M. F. Lappert*, and *R. Pearce*, J. Am. Chem. Soc. **99**, 6645 (1977); *K. Prout, T. S. Cameron, R. A. Forder, S. R. Critchley, B. Denton*, and *G. V. Rees*, Acta Crystallogr., Sect. B **30**, 2290 (1974); *J. R. Schmidt* and *D. M. Duggan*, Inorg. Chem. **20**, 318 (1981); *K. W. Muir*, J. Chem. Soc. A **1971**, 2663; *J. L. Atwood, W. E. Hunter, D. C. Hrncir, E. Samuel, H. Alt*, and *M. D. Rausch*, Inorg. Chem. **14**, 1757 (1975); *M. A. Bush* and *G. A. Sim*, ibid. **1971**, 2225; *M. F. Lappert, T. R. Martin, J. L. Atwood*, and *W. E. Hunter*, J. Chem. Soc., Chem. Commun. **1980**, 476.
[16] *J. W. Lauher* and *R. Hoffmann*, J. Am. Chem. Soc. **98**, 1729 (1976), and references cited therein.
[17] For simplicity we use the notation $y^2, xy, x, s \ldots$ etc. for $4d_{y^2}, 4d_{xy}, 5p_x$, 5s orbitals respectively, of Zr.
[18] p_π and p_σ are already appropriate linear combinations of Cl^- x and y AOs.
[19] The contour lines here and in all plots are for values of $\pm 0.2, 0.1, 0.05, 0.025, 0.0125, 0.005$ of the wavefunctions; solid(dashed)lines for positive (negative) values, nodal lines are also shown.
[20] It is this π-MO asymmetry, which is responsible for the different thermodynamic stability of acyl complex isomers like **9** and **10**: *R. Hoffmann, P. Hofmann*, and *K. Tatsumi*, unpublished results.
[21] *L. Libit* and *R. Hoffmann*, J. Am. Chem. Soc. **96**, 1370 (1974).
[22] There exists an interesting analogy between a Cp_2MX (d^0)fragment and a Li^+ in molecular structures due to electronic similarities. A known zirconio-ethylene complex, $(Cp_2ZrCl)_2(C_2H_4)$, adopts a structure similar to that calculated for 1,2-Dilithioethane. For this analogy see: *A. J. Kos, E. D. Jemmis, P. v. R. Schleyer, R. Gleiter, U. Fischbach*, and *J. A. Pople*, J. Am. Chem. Soc. **103**, 4996 (1981).
[23] *P. v. R. Schleyer, G. W. Spitznagel*, and *T. Clark*, private communication.
[24] While varying α, β, γ, we have kept the CH_2 and PH_2 hydrogens on the Zr–C–P and C–P–Zr bisector planes so that they followed the ring closure pathway. For η^1-minima the C–PH_2 fragment has been kept tetrahedral.

[25] For examples see: *P. C. Wailes, R. S. P. Coutts,* and *H. Weigold,* Organometallic Chemistry of Titanium, Zirconium, and Hafnium, Academic Press, N.Y. 1977.

[26] b_1 results from one member of the e_{1g}^* level of a D_{5h} Cp_2M by bending.

[27] For a useful representation of cyclopropane MOs see: *W. L. Jorgensen* and *L. Salem,* The Organic Chemists Book of Orbitals, Academic Press, N.Y. 1973.

[28] γ of course also varies if we interconvert the optimized η^1 and η^2-structures. The conclusions from the simplified pathway remain unchanged.

[29] *H. Basch, A. Viste,* and *H. B. Gray,* Theor. Chim. Acta **3**, 458 (1965). Charge iteration parameters from *V. I. Baranovskii* and *A. B. Nikol'skii,* Teor. Eksp. Khim. **3**, 527 (1967) [Chem. Abstr. **68**, 62802a (1968)].

[30] The competition by different π-donors for back donation to the metal has also been studied experimentally for CO insertions into Cp_2ZrMeX (X = Me, Cl, OEt) systems: *J. A. Marsella, K. G. Moloy,* and *K. G. Caulton,* J. Organomet. Chem. **201**, 389 (1980). A theoretical study is under way: *O. Eisenstein* and *P. Hofmann,* to be published.

[31] *K. I. Gell* and *J. Schwartz,* Inorg. Chem. **19**, 3207 (1980).

[32] *L. E. Manzer,* Inorg. Chem. **15**, 2567 (1976); *H. Schmidbaur, W. Scharf,* and *H.-J. Füller,* Z. Naturforsch., Teil B **32**, 858 (1977).

[33] *M. Pasquali, S. Gambarotta, C. Floriani,* and *A. Chiesi-Villa,* Inorg. Chem. **20**, 165 (1981).

[34] *S. Gambarotta, M. Pasquali, C. Floriani,* and *A. Chiesi-Villa,* Inorg. Chem. **20**, 1173 (1981).

[35] *B. Klei* and *J. H. Teuben,* J. Chem. Soc., Chem. Commun. **1978**, 659.

[36] Experimentally a precipitate of NaCl (about 85%) is observed. Quenching with D_2O of the reduced species at maximum ESR signal intensity stage produces Ph_2PCH_2D, showing that the Zr – C bond has not been cleaved by the 1-electron reduction process. *N. E. Schore,* unpublished results.

[37] *F. Calderazzo,* Angew. Chem. **89**, 305 (1977); Angew. Chem., Int. Ed. Engl. **16**, 299 (1977); *P. T. Wolczanski* and *J. E. Bercaw,* Acc. Chem. Res. **13**, 121 (1980); *R. S. Threlkel* and *J. E. Bercaw,* J. Am. Chem. Soc. **103**, 2650 (1981).

[38] *R. C. Fay* and *O. Eisenstein,* private communication. C – N rotation as an alternative process equilibrating the two methyl groups might occur here, however: *R. C. Fay,* unpublished. Also fluxional is $(Cp_2ZrCl)_2(OCHR)$ with two Cp_2ZrCl units complexing an aldehyde: *K. I. Gell* and *J. Schwartz,* J. Chem. Soc., Chem. Commun. **1980**, 550.

[39] *B. Longato, J. R. Norton, J. C. Huffman, J. A. Marsella,* and *K. G. Caulton,* J. Am. Chem. Soc. **103**, 209 (1981).

[40] *D. M. Hamilton jr., W. S. Willis,* and *G. D. Stucky,* J. Am. Chem. Soc. **103**, 4255 (1981). For a structure similar to **38**, $Cp_2Ti(OC)Co_3(CO)_9$, see: *G. Schmid, V. Bätzel, B. Stutte, M. Schneider,* and *E. Weiss,* J. Organomet. Chem. **113**, 67 (1976). Related is also $CpCo(CO)_2ZrCp_2$: *P. T. Barger* and *J. E. Bercaw,* ibid. **201**, C39 (1980).

[41] *R. Hoffmann,* J. Chem. Phys. **39**, 1397 (1963); *R. Hoffmann* and *W. N. Lipscomb,* J. Chem. Phys. **36**, 2179 (1962); **37**, 2872 (1962).

[42] *J. H. Ammeter, H.-B. Bürgi, J. C. Thibeault,* and *R. Hoffmann,* J. Am. Chem. Soc. **100**, 3686 (1978).

[43] *R. H. Summerville* and *R. Hoffmann,* J. Am. Chem. Soc. **98**, 7240 (1976).

[44] *T. A. Albright, P. Hofmann,* and *R. Hoffmann,* J. Am. Chem. Soc. **99**, 7546 (1977).

[374/81]